Unavoidable Geometric Errors in the Side Walls of End-milled Parts — Flat Surface —

Kang Kim*

School of Mechanical and Automotive Engineering, Kookmin University, 861-1 Jungreung-dong, Sungbook-gu, Seoul 136-702, Korea

A study for investigating the geometric characteristics of the side wall, which is generated by the flat end-milling process, is carried out through experiments and geometrical analysis. For this research, flat surfaces of prismatic parts are considered. It is assumed that the change of material removal per tooth causes the change of tool deflection. Under this assumption, it is verified that the milled surface geometry is directly affected by the amount of material removal per tooth. Analytical models for predicting the location, size, and depth of the geometrically defected zone are also developed.

Key Words : Flat End-milling Process, Geometric Errors of Side Wall, Cutting Conditions, Material Removal per Tooth

1. Introduction

It has been known that each manufacturing process generates characteristic surfaces inherently. For example, the centerless grinding process, which is used to manufacture cylindrical parts, is capable of producing a part of which cross sectional shape is a multi-arc polygon, having a constant diameter but not round (Rowe and Barash, 1964). A perfect cylinder can not be made by this process. Likewise, it has been found by machinists that the side wall of end-milled part shows gradually getting lower at the end of this surface as compared with the average surface line along the feed direction. This typical surface geometry, which can be easily ascertained through the straightness profile measurement of the end-milled side wall, is shown in Fig. 1. This geometrical surface error is caused from the surface generation mechanism of end-milling process itself. This error can be lessened by selecting optimal process variables, but not be eliminated completely without any other finishing process.

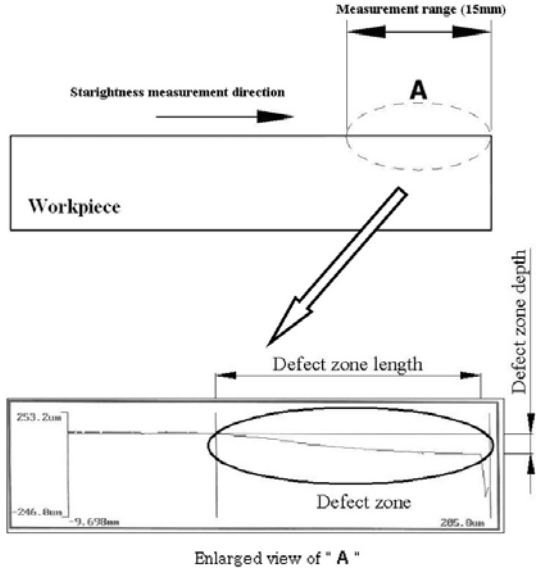

Fig. 1 Typical surface geometry of end-milled side wall

* Corresponding Author,
E-mail : kangkim@kookmin.ac.kr
TEL : +82-2-910-4676; **FAX** : +82-2-910-4839
School of Mechanical and Automotive Engineering, Kookmin University, 861-1 Jungreung-dong, Sungbook-gu, Seoul 136-702, Korea. (Manuscript **Received** October 9, 2006; **Revised** November 29, 2006)

The major independent variables in the end-milling process are related to the machine tool, tool, workpiece and cutting conditions. And the geometric features of milled surfaces are influenced by these variables (Budak and Altintas, 1994 ; Choi and Yang, 1998 ; Ko et al., 2001 ; Lee and Ko, 1999 ; Ryu et al., 2003 ; Tlusty et al., 1990 ; Yoon et al., 2003). These variables have direct relations with cutting forces and tool deflection. They are also important factors for getting precise end-milled surfaces (Cho and Yang, 1992 ; Kim and Ko, 2001 ; Seo and Cho, 1999a, 1999b) In most cases, the machine tool, tool and workpiece are predetermined before milling. The cutting conditions, such as cutting speed, feed rate and depth of cut, are the only variables that can be adjusted by an operator during milling. It is important to find the optimal cutting conditions in the view of the milled surface geometry when the machine tool, tool and workpiece are predetermined.

In this paper, the defect zone, where the end-milled side walls have geometric surface errors, is introduced and characterized by the length and the depth of it. Through the experimental end-milling process, the relationship between the defect zone and the cutting conditions is examined qualitatively and quantitatively. Then, an analytical model for expecting the size of unavoidable geometric error (the length and the depth of defect zone) under given cutting conditions is developed and verified based on the experimental results.

2. Defect Zone

A flat end mill has cutting edges not only at the end face of it but also along its circumference. The new bottom surface, which is perpendicular to the rotational axis of the end mill, and side wall, parallel to the rotational axis of it, are generated on the workpiece simultaneously. The flat end mill process can be used to produce flat surfaces along with various profiles and cavities. It is very difficult to understand the geometric errors of all kinds of end-milled shapes. As a first step, this study focuses on the flat side walls that are generated by unidirectional straight feeding in flat end-milling.

Figure 2 is the schematic illustration of the relative motion of end-milling tool in process. If the spindle speed, the feed rate and the apparent depth of cut are kept constant during process, the material removal per tooth increases gradually from zero to a certain value, then maintains this value, and finally decreases gradually from this value to zero. As a matter of convenience, portions of the side wall where the material removal per tooth increases, maintains a certain value, and decreases are named 'entry region' (I in Fig. 2), 'steady cutting region' (II in Fig. 2) and 'exit region' (III in Fig. 2) respectively. Each region is also defined as a location of the tool center or a projected location of the tool center on the side wall of the workpiece as shown in Fig. 2.

The typical straightness profile of the flat end-milled side wall is shown in Fig. 1. The straightness measurement direction is managed to be identical with the relative feed direction of tool. As shown in this figure, the tool generates flat surface at the entry region and steady cutting region. But, when the tool reaches the exit region, the surface is getting lower and lower compared to the surface of the other regions, and reaches to the lowest point at the end of process. Where the flatness of surface is relatively worse is named as 'defect zone'. And this defect zone is characterized as 'defect zone length' and 'defect zone depth'. It is presumed that there is an intimate relationship between the change of material removal per tooth during process and the defect zone.

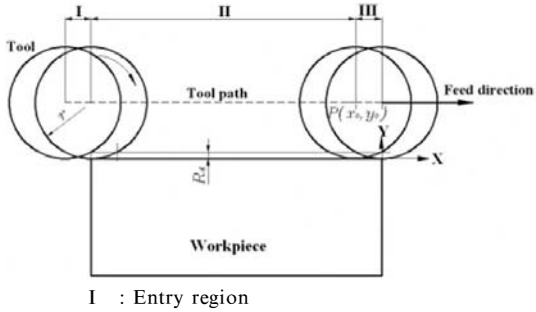

I : Entry region
II : Steady cutting region
III : Exit region

Fig. 2 Schematic illustration of the relative motion of end-milling tool

In end-milling process, the change of material removal per tooth during process is inevitable, even though the amount of the change of it may be reduced under the different cutting conditions. Likewise, there is a possibility that the defect zone length and depth can be minimized by optimal cutting conditions. But, the appearance of defect zone cannot be avoided.

3. Experiment

The goal of this experiment is to find the effects of the cutting conditions on the end-milled side wall, and to provide bases for developing analytical model of the defect zone. Fig. 3 shows the shape and size of specimens. They were hexahedra with horizontal slot, and made from a general purpose carbon steel (SM45C). To keep the same thickness for all specimens after the experimental milling process that has four different radial depth of cut conditions, the dimension L1 in Fig. 3 has four different values. The slot was also machined on the side wall to eliminate any effect of the cutting teeth of end-mill end face. To minimize differences in the surface geometry and condition between specimens, they were ground in the preparation process. The straightness of their side wall before the experiment has direct effect on the experimental results. So, nine specimens were sampled randomly, and measured straightness errors. Table 1 shows that the straightness errors were between 0.26~0.57 μm. It is expected that the straightness errors of specimens are much smaller than experimental results.

The CNC vertical milling machine used in the experiment was Model TMV-40M. The detail specification of this milling machine is provided in Table 2. Before the experiment, the accuracy of the machine table movement was measured and calibrated using Model AVEC-100 Ballbar system. Through this calibration, the errors of the machine table movement was kept less than 0.5 μm. Titanium coated standard 2 flutes high speed steel end-milling tools were used for the experiment. The diameter and the helix angle of them were 20 mm and 30° respectively. Tool wear may have affected the experiment. The tool was changed as a new one in every five experimental milling operation. In Fig. 4, the microscopic views of cutting edges in the new tool and in the worn tool after machining five specimens are shown.

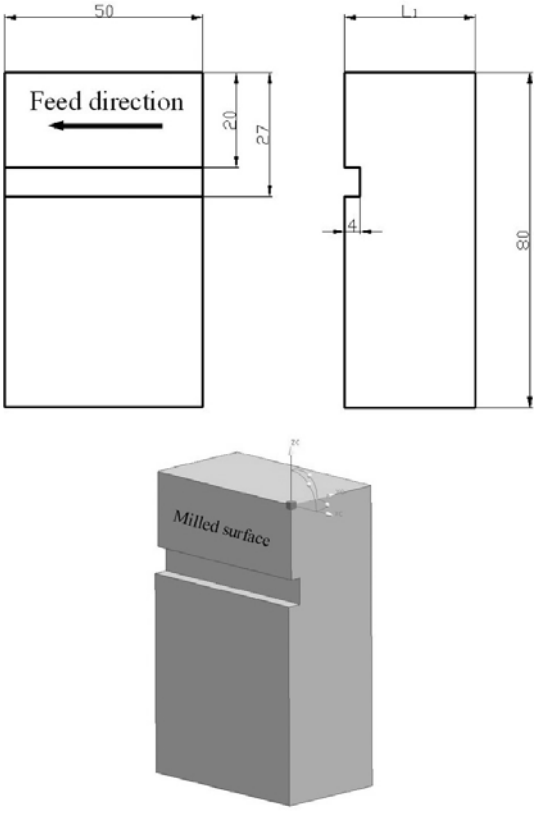

	Dimension
L1 (mm)	30.5, 31.0, 31.5, 32.0

Fig. 3 Specimen (unit : mm)

Table 1 Straightness error of specimen before experiment

(unit : μm)

	1	2	3	4	5	6	7	8	9	Average
Straightness error	0.41	0.35	0.29	0.34	0.57	0.39	0.26	0.34	0.29	0.36

Table 2 Specification of CNC milling machine

Table size (mm)		900×410
Traverse X, Y, Z axis (mm)		560×410×510
Spindle	Speed (rpm)	40~4000
	Taper	NT. 40
	Motor power (kW)	AC 5.5
Feed rate (mm)		1~5000
CNC		Fanuc 0M

Table 3 Specification of the measurement system (Talysurf Series 2)

Traverse Unit	
Measurement length (mm)	120
Speed of traverse (mm/sec)	0.5
Straightness of traverse (μm/sec)	0.5/120
Column	
Measurement length (mm)	450
Carriage traverse speed (mm/sec)	0.25~10
Speed of angular rotation of carriage (min/sec)	15~40
Range of carriage tilt adjustment (°)	±9
Material	Epoxy granite
Base	
Material	Epoxy granite
W×D×H (mm)	760×500×120
Features	2 tee-slots

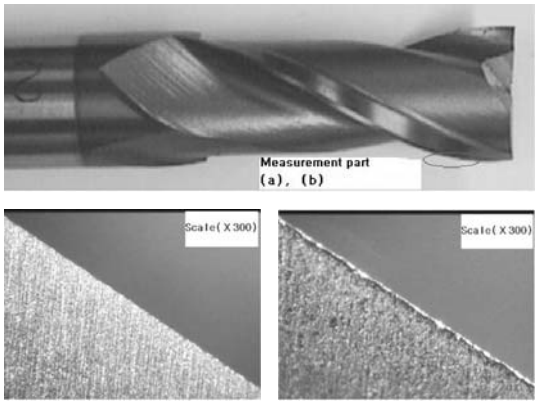

(a) New tool (b) After machining 5 specimens

Fig. 4 Tool wear

Table 4 Experimental conditions

Conditions	Value
Feed per tooth (mm/tooth)	0.09
Feed rate (mm/min)	70
Spindle speed (rpm)	381
Radial depth of cut, R_d (mm)	0.5, 1.0, 1.5, 2.0
Axial depth of cut, A_d (mm)	20
Tool revolution direction	Clockwise
Tool path	Down cut milling

The straightness profiles of the end-milled side walls were measured at the middle of side walls along the relative feed direction of tool by Form Talysurf Series 2 system. Table 3 shows the specification of it. As mentioned before, the defect zone locates around the exit region when the material removal per tooth is changing. In the exit region, the material removal per tooth is affected not only by cutting conditions but also by the tool radius. The only 15 mm range at the end of the side wall along the feed direction of tool was measured to get more detail information of the straightness profile (Fig. 1).

Table 4 shows experimental cutting conditions. The spindle speed, the feed rate and the axial depth of cut were set constant to be 381 rev/min, 70 mm/min and 20 mm respectively. The radial depth of cut was varied from 0.5 mm to 2.0 mm at 0.5 mm intervals.

4. Defect Zone Modeling

The end-milling process generates a new side wall in the order of entry region, steady cutting region and exit region. There must be some changes of the material removal per tooth in the entry and exit regions. This change of material removal per tooth causes cutting force to be varied. Normally the variation of cutting force leads to an error in the machined surface geometry because of the machining elasticity. When the tool is in the entry region, the newly generated surface is not the ultimate side wall because the consecutive cutting tooth always regenerates the surface. In this region the size of each chip is getting larger until the

cutting tooth reaches to the steady cutting region. And there is no change of the material removal per tooth in the steady cutting region. The size and shape of each chip in the steady cutting region are identical. The ultimate after-machined surface generated in the entry region and the steady cutting region has no geometrical error in ideal cases. But, in the exit region the size of each chip is getting smaller until it becomes zero. Thus, it is presumed that the exit region corresponds to the defect zone.

4.1 Defect zone length

Cartesian coordinate system is used in the analysis. As shown in Fig. 2, X-axis coincides with the after-machined surface of the side wall along the feed direction of the tool. And Y-axis is orthogonal to the X-axis. The exit region starts when the circumference of tool meets the end side of workpiece. It is assumed that $P(x_0, y_0)$ is the location of tool center at this instant. R_d and r mean the radial depth of cut and the tool radius respectively. Then, the relationship between x_0, y_0, R_d and r can be expressed as

$$r^2=x_0^2+(y_o-R_d)^2 \tag{1}$$

If there is no elastic deformation in any element of this system, it is assumed that y_0 is equal to r. So substituting this into Eq. (1), x_0 can be expressed as

$$x_0=-\sqrt{R_d(2r-R_d)} \tag{2}$$

The absolute value of x_0 is equivalent to the defect zone length, D_l. Thus D_l is

$$D_l=|x_0|=\sqrt{R_d(2r-R_d)} \tag{3}$$

4.2 Material removal per tooth

The material removal per tooth means the amount of workpiece material removed by a cutting tooth during the tool moves the distance that is equal to the feed per tooth, f_t. It is determined from the equation

$$f_t=\frac{F}{N\times Z} \tag{4}$$

where F is the feed speed of the workpiece, N is the rotational speed of the tool and Z is the number of teeth on the tool periphery. The total number of the material removal by every cutting tooth in the defect zone, n, is

$$n=INT\left\{\frac{|x_0|}{f_t}\right\} \tag{5}$$

If the tool center locates at $P(x_i, y_i)$ when the i^{th} material removal occurs in the defect zone, x_i, y_i and the angular displacement α_i in Fig. 5 can be expressed as

$$x_i=x_0+n\times f_t \quad (i=1,\cdots,n) \tag{6}$$

$$y_i=r \tag{7}$$

$$\alpha_i=\tan^{-1}\left|\frac{x_i}{\sqrt{(y_i^2-x_i^2)}}\right|=\tan^{-1}\left|\frac{x_i}{\sqrt{(r^2-x_i^2)}}\right| \tag{8}$$

Figure 6 shows that the area S_i corresponds to the amount of workpiece that would be removed just after the occurrence of the i^{th} material removal. To get S_i, it is decomposed into three elements, S_{i0}, S_{i1} and S_{i2}. They and S_i are as follows.

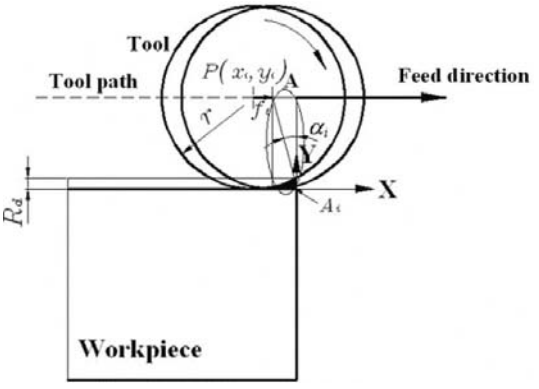

Fig. 5 Coordinate system

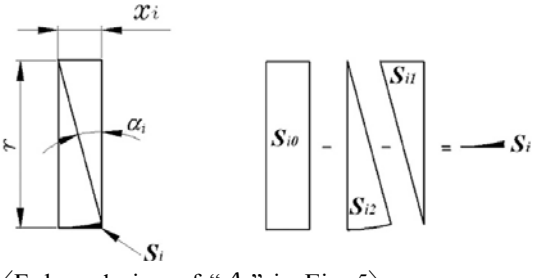

〈Enlarged view of "A_i" in Fig. 5〉

Fig. 6 Material to be removed after the i^{th} removal in exit region

$$S_{i0}=x_i\times r \tag{9}$$

$$S_{i1}=\frac{1}{2}x_i\times r\cos\alpha_i \tag{10}$$

$$S_{i2}=\frac{1}{2}r^2\times\alpha_i \tag{11}$$

$$S_i=S_{i0}-S_{i1}-S_{i2} \tag{12}$$

Therefore the material removal per tooth at the i^{th} occurrence in the defect zone, A_i can be expressed

$$A_i=S_{i-1}-S_i \quad (i=1,\cdots,n) \tag{13}$$

The initial value of the material removal per tooth, A_0, is equal to the material removal per tooth in the steady cutting region. It can be easily expressed as a function of the feed per tooth and the radial depth of cut in this region, as follows:

$$A_0=f_t\times R_d \tag{14}$$

4.3 Defect zone depth

Normally, the apparent depth of cut is greater than the true depth of cut. And, if the difference between them is larger, the defect zone depth looks deeper. This is caused by the effect of machine system rigidity and the cutting force. This has been known as 'machining elasticity' that was introduced in the study on the inherent accuracy of the centerless grinding process by Rowe and Barash (Rowe and Barash, 1964). For adapting the machining elasticity concept, a coefficient of machining elasticity, K, is defined as the ratio of true depth of cut to material removal per tooth, and expressed as

$$K=\frac{T_0}{A_0}=\frac{T_i}{A_i} \tag{15}$$

where T_0 is the initial value of the true depth of cut which is equal to the true depth of cut in the steady cutting region, and T_i is the true depth of cut at the i^{th} occurrence in the defect zone. The defect zone depth at the i^{th} occurrence in the defect zone, $(D_d)_i$, is the same as the difference between T_0 and T_i, and given as follows.

$$(D_d)_i=T_0-T_i=K(A_0-A_i) \tag{16}$$

It is very difficult to find the value of K theoretically, because it is affected by lots of factors. It is found by comparison between the simulation results using this defect zone model and the experimental results by trial and error.

5. Results and Discussions

5.1 Defect zone length

The measured experimental results on the defect zone length are compared with the predicted simulation results. As shown in Fig. 7, the differences between these results are less than ±5%. When the radial depth of cut increases from 0.5 mm to 2.0 mm at 0.5 mm intervals, the defect zone length is getting longer even though the increment is getting smaller slightly. The defect zone is corresponding to the overlapped area between a rec-

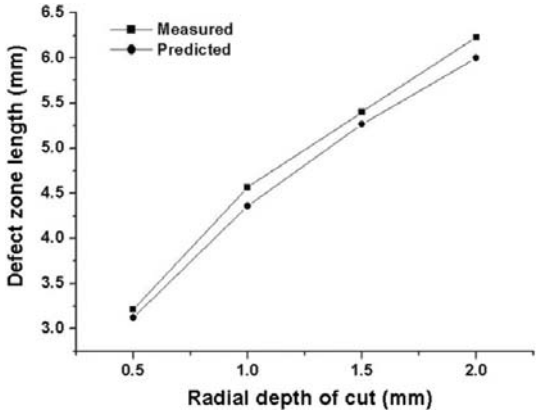

Fig. 7 Effect of radial depth of cut on defect zone length (Experiment and Simulation)

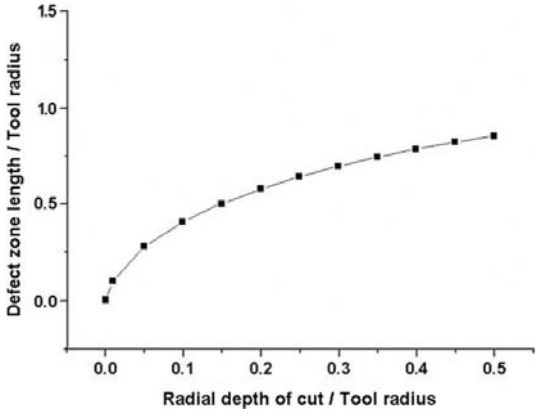

Fig. 8 Effect of radial depth of cut/radius of tool on defect zone length (Simulation)

tangular and a circle, when the centre of the circle with a radius equal to the value of tool radius is above the rectangular with a height equal to the value of radial depth of cut, and located on the extended vertical line of one end side, and the bottom side of the rectangular is in tangential contact with the circle. This means that not only the radial depth of cut but also the tool radius affects the defect zone length. Their effect can be ascertained in Fig. 8, which is a graph presenting the normalized Eq. (3) including the parameters divided by the tool radius. As expected, the defect zone is getting wider when the radial depth of cut increases, if the tool radius is greater than the radial depth of cut and constant. But, the increment of the defect zone length is relatively getting smaller, and it would be zero when the radial depth of cut is greater than the tool radius. When the tool radius decreases, the radial depth of cut per tool radius increases and the defect zone length per tool radius also increases. But, the decreasing rate of tool radius is much faster than the increasing rate of the defect zone length per tool radius. So, the defect zone shrinks when the tool is getting slenderer. The same trends can be easily found in the real end-milling process.

5.2 Defect zone depth

To complete the modeling of the defect zone depth, the coefficient of machining elasticity, K, in Eqs. (15) and (16) must be found. So, simulations were performed under the different conditions of value K. By comparing simulation results, it is concluded that K is 530 when the least square error between the measured and predicted profiles of defect zone is minimum. The predicted profiles in $K=530$ are compared with the measured profiles in Fig. 9. All the profiles in this figure have a common tendency to increase in depth gradually by the tool approaching the end side of workpiece, and to reach the maximum depth at the end side of workpiece when the tool leaves the workpiece always. Thus, the defect zone maximum depth can provide sufficient information on the side wall geometry with the defect zone length without any details on the profile. Figs. 10 and 11 show the effects of the tool radius, the radial depth of cut and the feed rate on the defect zone maximum depth. To help understanding on the milled-surface geometry, the defect zone depths are shown as negative (-) values in these figures. As shown in Fig. 10, the differences between the

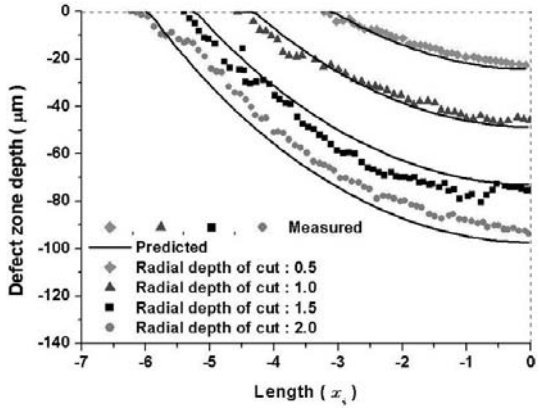

Fig. 9 Defect zone profile (Experiment and Simulation)

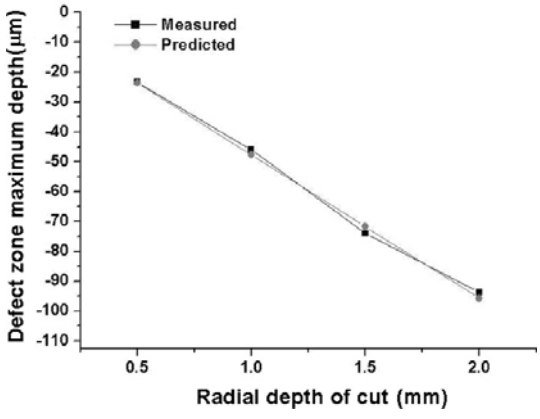

Fig. 10 Effect of radial depth of cut on defect zone max. depth (Experiment and Simulation)

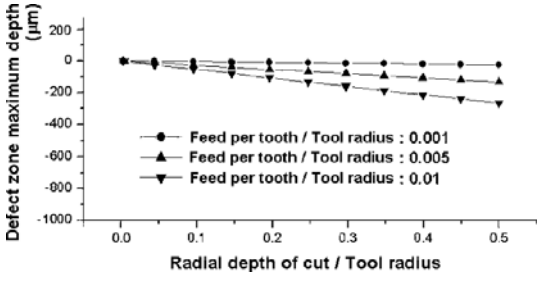

Fig. 11 Effect of radial depth of cut/radius of tool on defect zone max. depth (Simulation)

measured and predicted results of the defect zone maximum depth are less than ±4% when the radial depth of cut increased from 0.5 mm to 2.0 mm at 0.5 mm intervals. Equations in 4.2 reveal that the tool radius and the feed rate affect the material removal per tooth. They also have an effect on the defect zone maximum depth, and their effects are found in Fig. 11. As a matter of convenience, the feed per tooth and the radial depth of cut in Fig. 11 are presented as normalized values divided by the tool radius. Likewise the radial depth of cut, an increase in the feed per tooth makes the defect zone maximum depth deeper if the cutting conditions except the feed per tooth are unchanged. As mentioned before, the defect zone depth is caused by the machining elasticity. A relatively slenderer tool would generate a relatively deeper surface error on the side wall because of the elasticity of the tool. The same effect of the tool radius is induced from Fig. 11. As shown in this figure, the defect zone maximum depth may be over 100 μm in rough cutting. In this case, the consecutive fine cutting may be useless, because there is a possibility that the defect zone maximum depth after rough cutting is deeper than the depth of cut for fine cutting.

6. Conclusions

It has been known that the changes of material removal rates are related to the geometry of machined surface. In the flat end-milling process, the material removal rate must be changed from a certain value to zero when the tool leaves the workpiece. The existence of this leaving is directly related to unwanted generation of geometrically defected surface, which is named defect zone. The defect zone in the end-milled side wall is characterized by the length and the maximum depth, and affected by the radial depth of cut and the tool radius. The feed per tooth also has an effect on the defect zone maximum depth. To minimize the defect zone, it is recommended to decrease the radial depth of cut and the feed per tooth. The tool radius needs to be decided prudently because of the trade-off between the defect zone length and the defect zone maximum depth. Through the careful selection of cutting conditions, the defect zone may be lessened, but can not be eliminated or avoided, because there always be leaving of the tool from the workpiece.

Acknowledgments

This work was supported by research program 2004 of Kookmin University in Korea.

References

Budak, E. and Altintas, Y., 1994., "Peripheral Milling Conditions for Improved Dimensional Accuracy," *Int. J. Mach. Tools Manu.*, Vol. 34, No. 7, pp. 907～918.

Cho, H. D. and Yang, M. Y., 1992, "A Study on the Prediction of Tool Deflection and Precision Machining in Ball End Milling Process," *KSME Journal*, Vol. 16, No. 9, pp. 1669～1680.

Choi, J. G. and Yang, M. Y., 1998, "In-Process Prediction of the Surface Error Using an Identification of Cutting Depths in End Milling Operation by Simulating Surface," *J. of KSPE*, Vol. 15, No. 2, pp. 114～123.

Kim, Y. H. and Ko, S. L., 2001, "Improvement of the Accuracy in Cornering Cut Using End Mill," *KSME Journal*, Vol. 25/A, No. 3, pp. 399～407.

Ko, S. L., Lee, S. K. and Bae, S. M., 2001, "Study on the Design of End Mill Geometry," *J. of KSPE*, Vol. 18, No. 8, pp. 24～30.

Lee, S. K. and Ko, S. L., 1999, "Analysis on the Precision Machining in End Milling Operation by Simulating Surface Generation," *J. of KSPE*, Vol. 16, No. 4, pp. 229～236.

Rowe, W. B. and Barash, M. M., 1964, "Computer Method for Investigating the Inherent Accuracy of Centerless Grinding," *Int. J. Mach. Tool Des. Res.*, Vol. 4, pp. 91～116.

Ryu, S. H., Choi, D. K. and Chu, C. N., 2003, "Optimal Cutting Condition in Side Wall Milling Considering Form Accuracy," *J. of KSPE*, Vol. 20, No. 10, pp. 31～39.

Seo, T. I. and Cho, M. W., 1999a, "Tool Trajectory Generation Based on Tool Deflection Effects in Flat-End Milling Process (I)—Tool Path Compensation Strategy—," *KSME International*

Journal, Vol. 13, No. 10, pp. 738～751.

Seo, T. I. and Cho, M. W., 1999b, "Tool Trajectory Generation Based on Tool Deflection Effects in Flat-End Milling Process (II)—Prediction and Compensation of Milled Surface Errors—," *KSME International Journal*, Vol. 13, No. 12, pp. 918～930.

Tlusty, J., Smith, S. and Zamudia, C., 1990, "New NC routines for Quality in Milling," *Annals of CIRP*, Vol. 39/1, pp. 517～521.

Yoon, J. H., Cheong, M. S. and Lee, H. C., 2003, "A Study on Transition of Dimension Error and Surface Precision in High Speed Machining of Al-alloy," *J. of KSMTE*, Vol. 9, No. 3, pp. 96～102.